

First Physics with MPD Experiment at the NICA Accelerator Complex*

Vladimir D. Kekelidze, Adam Kisiel,[†] and Viacheslav Golovatyuk[‡]
Joint Institute for Nuclear Research, Dubna, Moscow Region, Russian Federation

(MPD Collaboration)
(Dated: January 10, 2020)

The Nuclotron-base Ion Collider fAcility (NICA) is in construction at the Joint Institute for Nuclear Research (JINR). The accelerator complex will consist of several components, specifically the Nuclotron accelerator, the Booster support accelerator, two ion sources, as well as the NICA collider ring with the corresponding transfer lines from Nuclotron. The expected date of putting the NICA collider ring in operation is N-th Month of 202X. At the same time the Multi-Purpose Detector (MPD) has been designed to operate at NICA. Components of MPD are currently in production. The assembly of the detector on-site is expected to start on M-th of Month of 202x, while on Month of 202x the detector setup will start the commissioning, to be ready for data taking on first beam from NICA.

This document details the preparation schedule for the construction and commissioning of MPD. It presents the plans for the first physics measurements at NICA and puts them into context of existing and planned physics experiments in the area of QCD phase diagram investigation.

I. THE NICA COMPLEX CONSTRUCTION SCHEDULE AND EXPECTED INITIAL PERFORMANCE

The NICA Accelerator complex progress is described in detail in XYZ. The expected date of the start of operation of NICA is Month of 202X. The initial luminosity is planned to be $X.y \cdot 10^{25} \text{ cm}^{-2} \text{ s}^{-1}$. Symmetric collisions of Au ions at $\sqrt{s_{NN}} = 10 \text{ GeV}$ will be performed in the initial stages of NICA operation.

II. READINESS OF THE MPD EXPERIMENT

A. Technical infrastructure and support systems

1. MPD Hall and facilities

The preparation of the MPD hall and support facilities. Power supply. Gas supply. Air-conditioning. External data transfer links. Liquid helium facilities and installation. MPD counting room.

2. MPD magnet

MPD Magnet preparation. External iron yoke assembly, installation and commissioning. Superconducting coil installation and commissioning. Integration with power supply and liquid helium installation. Magnetic field measurements.

3. MPD mechanical integration and support structure

Carbon-fiber mechanical structure for MPD detector component mechanical integration and installation. Beam pipe production and commissioning. Beam pipe integration and installation. Integration with NICA final focusing structure. Mechanical integration of forward detectors and laser systems. Integration with support systems.

4. Electronics support infrastructure

MPD Electronics Platform construction and integration. Integration of the Platform with external facilities - power supply, data interlinks, cabling for the experiment, control systems. Installation and commissioning of detector electronics and control systems on Platform.

B. Main MPD detector components for Stage 1

1. MPD Time Projection Chamber

Production, installation and commissioning of the MPD Time Projection Chamber. Calibration strategy for the TPC. Calibration with cosmic rays. Calibration with laser system. Internal and inter-subdetector alignment. Gas system installation and commissioning.

2. MPD Time Of Flight

Production, installation and commissioning of the MPD Time Of Flight detector. Calibration strategy for the TOF detector. Gas system installation and commissioning. Calibration with cosmic rays.

* A report for the Scientific Council of JINR

[†] Also at Faculty of Physics, Warsaw University of Technology, Warsaw, Poland.

[‡] Second.Author@institution.edu

67	3. <i>MPD Electromagnetic Calorimeter</i>	104
68	Strategy for MPD Electromagnetic Calorimeter pro-	106
69	duction and staged installation procedure and schedule.	
70	ECAL calibration strategy. Commissioning of installed	
71	ECAL components. Calibration with cosmic rays.	107
72	4. <i>MPD Hadronic Calorimeter</i>	108
73	Production, installation and commissioning of the	109
74	MPD Hadronic Calorimeter. Calibration strategy for the	110
75	HCAL.	111
		112
76	5. <i>Fast Forward Detector</i>	113
		114
		115
77	Production, installation and commissioning of the	116
78	MPD Fast Forward Detector. Calibration strategy for	117
79	FFD. Integration of FFD with beam diagnostics and	118
80	monitoring.	
81	6. <i>MPD Cosmic Ray Detector</i>	119
		120
82	Design, production, installation, and commissioning of	
83	the MPD Cosmic Ray Detector (MCORD). Strategy for	121
84	subdetector component calibration with MCORD mod-	122
85	ules on-site and in testing laboratories. Trigger strategy	123
86	for MCORD.	124
		125
		126
87	C. MPD Electronics	127
		128
88	1. <i>Slow Control System</i>	
89	Project, installation and commissioning of the MPD	
90	Slow Control System. Plan for monitoring of detector	129
91	operation. Error reporting and alarm handling proce-	
92	dures for detector subsystems and experiment. Interface	130
93	for detector monitoring and control for experiment oper-	131
94	ators.	132
		133
		134
95	2. <i>Data Acquisition</i>	135
		136
96	Project, installation and commissioning of Data Ac-	137
97	quisition System. Strategy for data integration from de-	
98	detector subsystems. Computing and data transfer require-	
99	ments for the DAQ.	
		138
100	3. <i>Experiment control system</i>	139
		140
101	Project, installation and commissioning for the Exper-	141
102	iment Control System. Integration of the Subsystems,	142
103	Slow Control and DAQ subsystems. Unified, integrated	143

control system for MPD. Interface for the MPD experts and operators. Instruction for experimental shift crew for standard detector operation during running periods.

D. Summary timeline of detector readiness

III. TRIGGERING AND DATA RATE

Plan for the triggering system for MPD. Structure for determination of triggering algorithms and triggering priorities. Implementation of the trigger mix and instructions for detector operators.

Expected data rate for initial operation of the MPD is of the order of 100 Hz. With reasonable safety margin and initial machine commissioning phase it is expected that data sample collected in the first week of MPD operation will be of the order of 10 million minimum-bias events.

IV. COMPUTING AND SOFTWARE REQUIREMENTS

Main computing facilities for MPD data handling and storage, reconstruction, data analysis and Monte-Carlo simulations. Integration of the computing resources of Laboratory for Information Technology, the NICA Cluster at the Laboratory of High Energy Physics, as well as external computing resources in MPD member institutions. Estimation of the computing resources needed for full data reconstruction and analysis.

A. MPD Computing

Computing resources for MPD. Current status and installation plans. Integration of computing and data transfer infrastructure. Plan for transfer of storage of experimental data from the beam. Estimation of computing requirements for first-day data handling, calibration, production, and analysis. Mass storage and long-term storage of MPD experimental data. *** Oleg Rogachevsky, Boris Shchinov ***

B. MPD Software

Preparation of MPD software for data handling, calibration, and reconstruction. Status of the Monte-Carlo simulation of the MPD detector response. Preparation of data analysis software for day-one physics observables. *** Oleg Rogachevsky ***

C. Preparation for data taking and analysis

Schedule for large-scale Monte-Carlo production of data. Selection of event generators for simulations. Verification of the calibration procedures and data reconstruction. Preparation of analysis codes for first-day physics observables. Development of novel theories and model codes for simulation of interesting physics observables. *** All, AK, Oleg Rogachevsky ***

- preparation of software framework for run-by-run calibration of each detector and storage of the corresponding calibrations in the centralized database + support/maintenance/regular backup etc. The database should be able to service thousands of simultaneous connections.
- preparation of software framework for run-by-run quality assurance and data checks, defective runs should be stopped and rejected, existing problems fixed.
- reconfiguration of the existing reconstruction software to work with real data, so far it is tuned to work with simulations only, it does not know anything about the databases, calibrations etc.

D. Summary timeline for software and computing readiness

V. PHYSICS GOALS

Current status of investigation of QCD matter at extreme baryonic densities. Connection to physics of neutron star structure as well as neutron star collisions. Open questions in the investigation of QCD matter, the deconfined phase, the existence and nature of the phase transition from deconfined to hadronic matter, the conjectured critical point in the phase diagram. Recent theoretical developments. Relevance of specific Monte-Carlo event generator codes to the physics open questions. Identification of key first-day physics observables which could have the most impact on these investigations. Status of current and planned experimental efforts in similar collision energy range at other facilities and the relevance of MPD for these investigations. *** All, AK ***

VI. PLANS FOR FIRST-DAY MPD PHYSICS

A. Calibration and alignment

Strategy and schedule for assessment of detector calibration readiness for physics analyses. Estimation of uncertainties resulting from initial mis-calibration and mis-alignment of the detector. Strategy for detector calibration using cosmic ray running, detector component tests,

test-beam data, and Monte-Carlo simulation of detector response. Estimation of measurement potential for specific observables in variants of detector setup (partial detector installation, not fully calibrated subdetectors, etc).

B. Key first-day observables

Identification of observables with major physics message impact, which can be measured with initial first-day data sample. Strategy for preparation of data sample, data analysis code and independent verification of results within the MPD Collaboration. Strategy for timely preparation of the manuscripts with key measurements for rapid publication. Estimated impact of the key measurements for general landscape of QCD phase diagram studies. *** All, AK ***

Possible first-day observables include:

- h +/- multiplicity and E_T distributions – global parameters, comparison to earlier measurements – Feofilov/Adam?
- h +/- and π /K/p spectra vs. centrality – dN/dy , $\langle p_T \rangle$, R_{cp} , radial flow, horn, statistical models and μ/T - Vadim?
- flow h/π /K/p – wealth of physics – Arkadij?
- first results for multistrange baryons (Λ , Ξ , Ω) – strangeness - A. Zinchenko?
- some of basic resonances (ϕ , K^* , ρ) – hadronic phase, hadrochemistry – me?

Cross checks:

- π^0 , unlikely but possible – cross check with $\pi^{+/-}$ – me?
- $K_s \rightarrow \pi^+\pi^-$, quite possible – cross check with $K^{+/-}$ – A.Zinchenko?

1. Two-pion intensity interferometry

Intensity interferometry, usually referred to as "femtoscopia" is used extensively in heavy-ion collision studies to determine the size of the particle-emitting region as well as the details of the spatio-temporal dynamics of the system evolution[1–6]. In particular two-pion measurements are straightforward to perform due to the high statistics of pions as well as well understood methodology. The technique of the correlation function used in the measurements is, to the first order, insensitive to single particle acceptance effects, so it does not have strict requirements on the precision of the calibration process. At the same time it provides critical and sensitive probe

of the two-particle tracking and PID efficiency. As a result, measurement of the two-pion femtoscopic correlation functions is usually among the first performed at accelerator complexes immediately after their turn-on and as such, are excellent candidates for "First Physics" measurements.

Femtoscopic measurements have been performed for several decades, as a function of collision energy, collision system, collision centrality, pair transverse momentum, reaction plane orientation and more [7, 9–24]. A dependence of pion interferometry sizes on collision energy is of particular interest here. It has been argued [25] that a first-order phase transition will extend the lifetime of the system created in a heavy-ion collision, An expanding system living longer, will naturally reach larger size at freeze-out. This size is measured by pion femtoscopy. Therefore, measuring the size of the colliding system, in the NICA collision energy range is a crucial ingredient of the search for the existence and nature of the phase transition deconfined and hadronic matter.

Figure 1 shows the current world data on the pion freeze-out volume in heavy-ion collisions. Measurements at energies above 7.7 GeV are performed with detectors in collider geometry, but the results at the lower energy range suffer from limited statistics. Measurements at lower energies are performed in fixed-target experiments. Data from the AGS (E895 and E866) are several decades old, and were not analyzed with modern femtoscopic techniques. A rather striking non-monotonic behavior of the volume is observed in the NICA energy range, however it is unclear whether it can be explained by systematic uncertainties. A more precise data, based on large-statistics data sample in collider geometry experiment and analyzed with modern techniques is clearly necessary. MPD is best suited to provide this data in the

near future.

Femtoscopic size of the system can be measured in three directions in the so-called Bertsh-Pratt decomposition: "long" along the beam axis, "out" along the transverse momentum of the pair, and "side" perpendicular to the other two. It is argued, that emission duration affects strongly the size of the system in the direction of collective flow (associated with the "out" direction), while the "side" direction is unaffected. Analyzing the $R_{out}^2 - R_{side}^2$ is proposed as a sensitive probe of the duration of the particle emission stage. In particular the existence of the deconfined phase and the phase transition might affect this ratio strongly. Measuring this ratio can potentially give critical signatures of such transition. Figure 2 shows the values of this ratio measured to data in heavy-ion collisions. It is apparent that at in the range of collision energies of NICA potentially non-trivial behavior is observed. Unfortunately different experiments show strongly varying results. Due to significant systematic uncertainties of those measurements firm conclusions cannot be drawn from data collected so far. It is therefore of utmost importance to perform these measurements in MPD in collider geometry, with similar systematics and significant statistics across all collision energies, as well as with modern analysis techniques.

In light of the arguments given above specific analyses are foreseen for the first-day physics with a sample of up to 10 million minimum-bias events. Two-particle femtoscopic correlations for positively and negatively charged pions will be measured and sizes of the system at freeze-out will be inferred from them. A difference between them will be investigated, as data from lower energies (HADES experiment [24]) show clear differences in system size between π^+ and π^- while at higher energies (STAR and ALICE) no such difference is observed. Sizes

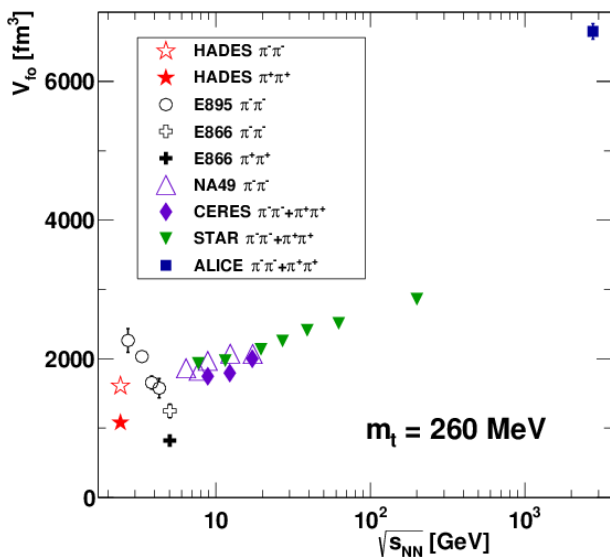


FIG. 1. Dependence of the freeze-out volume for pions on the collision energy. Compilation taken from [24]

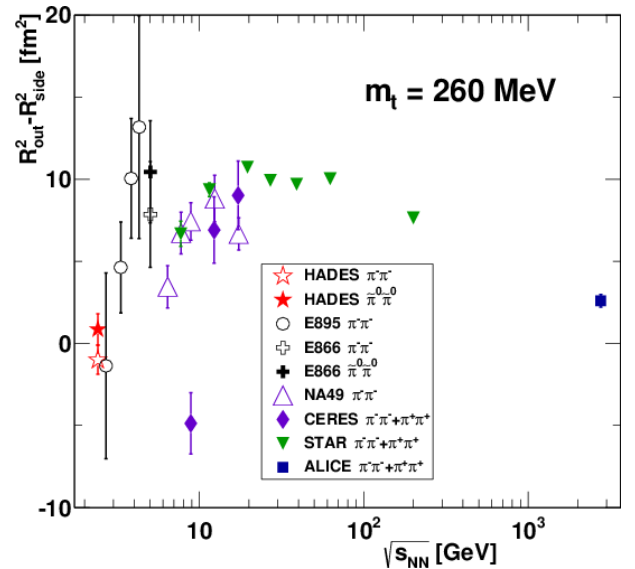


FIG. 2. The $R_{out}^2 - R_{side}^2$ dependence on collision energy. Compilation taken from [24]

will be extracted as a function of transverse momentum of the pair k_T (or the so-called "transverse mass" of the pair $m_T = \sqrt{k_T^2 + m_\pi^2}$. Decrease of the size with m_T is interpreted as a sign of collective expansion [26]. The measurement will also be done as a function of collision centrality. A scaling of the source size with charged particle multiplicity density is expected.

Initial Monte-Carlo simulations for the femtoscopic measurements at MPD have already been performed [25]. Measurement of the two-particle correlation for pions requires efficient particle tracking and momentum determination, which will be achieved at MPD, as described in Sections II B 1 and IV B. The TPC detector will provide critical information here. In addition the efficient particle identification will be crucial. Here again, the properly calibrated data on specific ionization energy loss $\langle dE/dx \rangle$ in the TPC gas will be used. In addition, at higher transverse momenta, additional information of the particle's time of flight from the TOF detector, described in Section II B 2, will be used to distinguish pions from kaons and heavier baryons. The design performance of the detector is expected to be more than adequate for the measurement. Analysis is expected to include the full statistics, no dedicated trigger is needed.

Two-particle correlations for identical particles (such

as $\pi\pi$ correlations discussed here) at low relative momentum are particularly sensitive to correlated two-particle efficiency of the detector. The pairs of particles of interest will have trajectories, which are close to each other in the TPC detector, and as a consequence can suffer from loss of efficiency, which is dependent on relative momentum. This effect is distinctively different and independent from single-particle efficiency. Therefore dedicated test of the reconstruction procedure are performed in order to understand the extent to which this effect is present. Specific correction procedures will be proposed, based on similar ones used in STAR and ALICE, which will first be tested on Monte-Carlo data and then validated on real data. Other corrections, such as momentum resolution correction, PID efficiency correction will also be applied. Since the measurement involves full minimum-bias sample with no specific data selection, all the analysis procedures will be prepared based on general-purpose large scale Monte-Carlo productions, with models such as UrQMD, vHELLE, Therminator2 and any other general-purpose model.

C. Summary timeline for first-day physics results publication

-
- [1] G. I. Kopylov and M. I. Podgoretsky, Correlations of identical particles emitted by highly excited nuclei, *Sov. J. Nucl. Phys.* **15**, 219 (1972), [*Yad. Fiz.*15,392(1972)].
- [2] G. I. Kopylov and M. I. Podgoretsky, The Interference of Two-Particle States in Particle Physics and Astronomy, *Zh. Eksp. Teor. Fiz.* **69**, 414 (1975), [,42(1975)].
- [3] M. I. Podgoretsky, Interference Correlations of Identical Pions: Theory. (In Russian), *Fiz. Elem. Chast. Atom. Yadra* **20**, 628 (1989).
- [4] R. Lednicky, Correlation femtoscopy of multiparticle processes, *Phys. Atom. Nucl.* **67**, 72 (2004), [*Yad. Fiz.*67,73(2004)], arXiv:nucl-th/0305027 [nucl-th].
- [5] S. Pratt, Pion Interferometry for Exploding Sources, *Phys. Rev. Lett.* **53**, 1219 (1984), [,160(1984)].
- [6] M. A. Lisa, S. Pratt, R. Soltz, and U. Wiedemann, Femtoscopy in relativistic heavy ion collisions, *Ann. Rev. Nucl. Part. Sci.* **55**, 357 (2005), arXiv:nucl-ex/0505014 [nucl-ex].
- [7] C. Adler *et al.* (STAR), Pion interferometry of $s(NN)^{1/2} = 130$ -GeV Au+Au collisions at RHIC, *Phys. Rev. Lett.* **87**, 082301 (2001), arXiv:nucl-ex/0107008 [nucl-ex].
- [8] K. Aamodt *et al.* (ALICE), Two-pion Bose-Einstein correlations in pp collisions at $\sqrt{s} = 900$ GeV, *Phys. Rev. D* **82**, 052001 (2010), arXiv:1007.0516 [hep-ex].
- [9] K. Aamodt *et al.* (ALICE), Two-pion Bose-Einstein correlations in central Pb-Pb collisions at $\sqrt{s_{NN}} = 2.76$ TeV, *Phys. Lett.* **B696**, 328 (2011), arXiv:1012.4035 [nucl-ex].
- [10] K. Aamodt *et al.* (ALICE), Femtoscopy of pp collisions at $\sqrt{s} = 0.9$ and 7 TeV at the LHC with two-pion Bose-Einstein correlations, *Phys. Rev. D* **84**, 112004 (2011), arXiv:1101.3665 [hep-ex].
- [11] B. B. Abelev *et al.* (ALICE), Two- and three-pion quantum statistics correlations in Pb-Pb collisions at $\sqrt{s_{NN}} = 2.76$ TeV at the CERN Large Hadron Collider, *Phys. Rev. C* **89**, 024911 (2014), arXiv:1310.7808 [nucl-ex].
- [12] B. B. Abelev *et al.* (ALICE), Freeze-out radii extracted from three-pion cumulants in pp , p-Pb and Pb-Pb collisions at the LHC, *Phys. Lett.* **B739**, 139 (2014), arXiv:1404.1194 [nucl-ex].
- [13] J. Adam *et al.* (ALICE), Two-pion femtoscopy in p-Pb collisions at $\sqrt{s_{NN}} = 5.02$ TeV, *Phys. Rev. C* **91**, 034906 (2015), arXiv:1502.00559 [nucl-ex].
- [14] J. Adam *et al.* (ALICE), One-dimensional pion, kaon, and proton femtoscopy in Pb-Pb collisions at $\sqrt{s_{NN}} = 2.76$ TeV, *Phys. Rev. C* **92**, 054908 (2015), arXiv:1506.07884 [nucl-ex].
- [15] J. Adam *et al.* (ALICE), Centrality dependence of pion freeze-out radii in Pb-Pb collisions at $\sqrt{s_{NN}} = 2.76$ TeV, *Phys. Rev. C* **93**, 024905 (2016), arXiv:1507.06842 [nucl-ex].
- [16] D. Adamova *et al.* (ALICE), Azimuthally differential pion femtoscopy in Pb-Pb collisions at $\sqrt{s_{NN}} = 2.76$ TeV, *Phys. Rev. Lett.* **118**, 222301 (2017), arXiv:1702.01612 [nucl-ex].
- [17] S. Acharya *et al.* (ALICE), Azimuthally-differential pion femtoscopy relative to the third harmonic event plane in Pb-Pb collisions at $\sqrt{s_{NN}} = 2.76$ TeV, *Phys. Lett.* **B785**, 320 (2018), arXiv:1803.10594 [nucl-ex].
- [18] J. Adams *et al.* (STAR), Three pion HBT correlations in relativistic heavy ion collisions from the STAR experiment, *Phys. Rev. Lett.* **91**, 262301 (2003), arXiv:nucl-

- ex/0306028 [nucl-ex]. 433
- [19] J. Adams *et al.* (STAR), Pion interferometry in Au+Au collisions at $S(NN)^{1/2} = 200$ -GeV, Phys. Rev. **C71**, 044906 (2005), arXiv:nucl-ex/0411036 [nucl-ex]. 435
- [20] B. I. Abelev *et al.* (STAR), Identified particle production, azimuthal anisotropy, and interferometry measurements in Au+Au collisions at $s(NN)^{1/2} = 9.2$ - GeV, Phys. Rev. **C81**, 024911 (2010), arXiv:0909.4131 [nucl-ex]. 437
- [21] B. I. Abelev *et al.* (STAR), Pion Interferometry in Au+Au and Cu+Cu Collisions at RHIC, Phys. Rev. **C80**, 024905 (2009), arXiv:0903.1296 [nucl-ex]. 438
- [22] M. M. Aggarwal *et al.* (STAR), Pion femtoscopy in p^+p collisions at $\sqrt{s} = 200$ GeV, Phys. Rev. **C83**, 064905 (2011), arXiv:1004.0925 [nucl-ex]. 439
- [23] L. Adamczyk *et al.* (STAR), Beam-energy-dependent two-pion interferometry and the freeze-out eccentricity of pions measured in heavy ion collisions at the STAR detector, Phys. Rev. **C92**, 014904 (2015), arXiv:1403.4972 [nucl-ex]. 440
- [24] J. Adamczewski-Musch *et al.* (HADES), Identical pion intensity interferometry in central Au + Au collisions at 1.23 A GeV, Phys. Lett. **B795**, 446 (2019), arXiv:1811.06213 [nucl-ex]. 441
- [25] D. Wielanek, P. Batyuk, R. Lednicky, O. Rogachevsky, I. Karpenko, L. Malinina, and K. Mikhaylov, Femtoscopy Studies at NICA Energy Scale, *Proceedings, 11th Workshop on Particle Correlations and Femtoscopy and NICA Days 2015 (WPCF 2015): Warsaw, Poland, November 3-7, 2015*, Acta Phys. Polon. Supp. **9**, 341 (2016). 442
- [26] V. A. Averchenkov, A. N. Makhlin, and Yu. M. Sinyukov, Study of Collective Motion in Hadronic Matter by a Pion Interferometry Method, Sov. J. Nucl. Phys. **46**, 905 (1987), [Yad. Fiz.46,1525(1987)]. 443